



ORIGINAL ARTICLE

# Synthesis, characterization and biological studies of some Co(II), Ni(II) and Cu(II) complexes derived from indole-3-carboxaldehyde and glycylglycine as Schiff base ligand

R. Selwin Joseyphus, M. Sivasankaran Nair \*

Department of Chemistry, Manonmaniam Sundaranar University, Tirunelveli 627 012, India

Received 15 May 2010; accepted 31 May 2010

Available online 4 June 2010

## KEYWORDS

Schiff base;  
IR;  
Conductance;  
XRD;  
SEM;  
DNA

**Abstract** The Schiff base ligand derived from indole-3-carboxaldehyde(indal) and glycylglycine(glygly) were synthesized and characterized by elemental analysis, IR, electronic spectrum,  $^1\text{H}$  NMR and mass spectrum. Co(II), Ni(II) and Cu(II)–indal-glygly Schiff base complexes were synthesized and characterized by elemental analysis, molar conductance, IR, electronic spectra, magnetic measurements, ESR, electrochemical studies, TGA, DSC analysis, XRD and SEM. Conductance measurements indicate that the above complexes are 1:1 electrolytes. IR spectral data show that the ligand is tridentate and the binding sites are azomethine nitrogen, peptide nitrogen and carboxylato oxygen atoms. Electronic spectral measurements indicate tetrahedral geometry for Co(II) and Ni(II) complexes and square planar geometry for Cu(II) complex. Magnetic measurements show weak ferromagnetic behaviour for Co(II) and Ni(II) complexes and paramagnetic behaviour for Cu(II) complex. ESR spectral data shows the ionic link between metal and the Schiff base ligand. The metal complexes are found to be stabilized in the unusual oxidation states of the metal ion during electrolysis. Thermal analysis of the complex indicates that the decomposition takes place in three steps. IR and thermal studies indicate that the fourth position would be occupied by a water molecule in complexes. XRD shows that the complexes have the crystallite size of 31, 40 and 67 nm, respectively. The surface morphology of the complexes was studied by SEM. The antimicrobial activity of the ligand and its complexes were screened by Kirby Bayer Disc Diffusion

\* Corresponding author. Tel.: +91 462 233387.

E-mail address: msnairchem@rediffmail.com (M. Sivasankaran Nair).



method. DNA cleavage studies were performed for metal–Schiff base complexes in presence of hydrogen peroxide as oxidant.

© 2010 King Saud University. All rights reserved.

## 1. Introduction

Schiff bases have played a special role as chelating ligands in main group and transition metal coordination chemistry because of their stability under a variety of redox conditions and because imine ligands are borderline Lewis bases (De Souza et al., 2003). The important physical and biological properties of the Schiff bases are directly related to intermolecular hydrogen bonding and proton transfer equilibria (Przybylski et al., 2002). Schiff bases also offer opportunities for inducing substrate chirality, tuning metal-centered electronic factors and enhancing the solubility and stability of homogenous or heterogeneous catalysts (Kannan and Ramesh, 2005). Transition metals are involved in many biological processes which are essential to life process. The metals can coordinate with *O*- or *N*-terminals from proteins in a variety of models and play a crucial role in the conformation and function of biological macromolecules (Colacio et al., 2000; Karaliota et al., 2001).

In the area of bioinorganic chemistry, interest in Schiff base complexes has centered on the role of such complexes in providing synthetic models for the metal-containing sites in metallo-proteins and metallo-enzymes (Mascharak, 2002). Indole and its derivatives are widely used in making perfumes, dyes, agrochemicals and medicines. Furthermore, tetradentate and tridentate Schiff base complexes are increasingly important for designing metal complexes related to synthetic and natural oxygen carriers. Copper complexes of tridentate Schiff base type especially with dimeric units are considered as bioinorganic model compounds. During the recent years there have been intense investigations of different classes of indole derivative compounds. Many of these possess interesting biological properties such as antimicrobial and analgesic activities. The important criteria for the development of metallodrugs as chemotherapeutic agents are the ability of the metallo drug to bring about DNA cleavage. A large number of transition metal complexes because of their redox properties, have been found to promote DNA cleavage.

Recently, we have reported some Schiff base metal complex systems (Nair et al., 2007; Joseyphus et al., 2006; Joseyphus and Nair, 2008; Nair and Joseyphus, 2008). In this study, we report the synthesis, characterization and antimicrobial and DNA cleavage studies of some mononuclear Co(II), Ni(II) and Cu(II) complexes of Schiff base ligand derived from indole-3-carboxaldehyde and glycylglycine.

## 2. Experimental

### 2.1. Materials and reagents

The commercially available glycylglycine was purchased from Fluka, indole-3-carboxaldehyde was obtained from Lancaster and metal(II) nitrates were obtained from Merck. All other reagents and solvents were purchased from commercial sources and were of analytical grade. Solvents were purified and dried by standard methods (Vogel, 1978).

### 2.2. Synthesis of Schiff base ligand

Glycylglycine (1 mmol) was dissolved in 20 cm<sup>3</sup> of methanol containing KOH (1 mmol). A solution of indole-3-carboxaldehyde (1 mmol) in 10 cm<sup>3</sup> of absolute methanol was added dropwise with stirring and refluxed for 2 h. The volume of the yellow solution was cooled at room temperature and then reduced *in vacuo* using a rotary evaporator. Anhydrous ether was added to deposit a yellowish precipitate, which was then recrystallized from ethanol.

### 2.3. Synthesis of Schiff base metal complexes

Schiff base ligand (1 mmol) was dissolved in 10 cm<sup>3</sup> of methanol and aqueous Co(II)/Ni(II)/Cu(II) nitrate (1 mmol) solution was added dropwise into 20 cm<sup>3</sup> of methanol. The resulting mixture obtained was stirred for 2 h. After allowing it to stand in air at room temperature the precipitated complex was filtered off, washed several times with cold ethanol, ether and then dried *in vacuo* over anhydrous CaCl<sub>2</sub>.

### 2.4. Instruments

Elemental analysis was performed using a Perkin–Elmer elemental analyzer. Metal contents present in the complexes were determined by EDTA titration. Molar conductance of the complexes was measured in DMSO solutions using a coronation digital conductivity meter. IR spectra were recorded in KBr disc on a JASCO FT/IR-410 spectrometer in the 4000–400 cm<sup>-1</sup> region. The electronic spectra were recorded on a Perkin–Elmer Lambda-25 UV–Visible spectrometer. The 400 MHz <sup>1</sup>H NMR spectrum of the Schiff base ligand was recorded in JEOL GSX 400 FT NMR spectrometer using tetramethylsilane as internal standard. The FAB-mass spectrum of the Schiff base ligand was recorded on a JEOL SX 102/DA-6000 mass spectrometer/Data system using Argon/Xenon (6 kV, 10 mA) as the FAB-gas. The accelerating voltage was 10 kV and the spectrum was recorded at room temperature using *m*-nitrobenzylalcohol as the matrix. Magnetic susceptibility measurements of the powdered complexes were carried out by employing the Guoy's method at room temperature. Copper sulphate was used as calibrant. Room temperature magnetic measurements were performed on an EG & G PARC vibrating sample magnetometer with a maximum applied field of 7 Oe. X-band ESR spectra of Cu(II) complexes were recorded on a Varian E112 X-band spectrometer. Electrochemical studies were carried out on a Bio Analytical System CV-50W electrochemical analyzer. The tetrabutylammonium perchlorate was used as the supporting electrolyte. Thermal studies were recorded on a Perkin–Elmer 7 series thermal analyzer, with a heating rate of 10 °C/min using N<sub>2</sub> atmosphere. XRD was recorded on a Rigaku Dmax X-ray diffractometer with CuK<sub>α</sub> radiation ( $\lambda = 1.5404 \text{ \AA}$ ). SEM images were recorded in a Hitachi SEM analyzer.

### 2.5. Antimicrobial studies

Antibacterial and antifungal activity of the ligand and its metal complexes were tested *in vitro* against the bacterial species *S. aureus*, *E. coli*, *K. pneumoniae*, *P. vulgaris* and *P. aeruginosa* and the fungal species *C. albicans*, *R. stolonifer*, *A. flavus*, *A. niger* and *R. bataticola* by Kirby Bayer Disc Diffusion method (Bayer et al., 1996). Amikacin, ofloxacin and ciprofloxacin were used as the standard antibacterial agents whereas nystatin was used as the standard antifungal agent. The test organisms were grown on nutrient agar medium in petri plates. Discs were prepared and applied over the long culture. The compounds were prepared in DMSO and soaked in filter paper disc of 5 mm diameter and 1 mm thickness. The concentrations of ligand and the complexes used in this study was 0.01 µg/ml. The discs were placed on the previously seeded plates and incubated at 37 °C and the diameter of inhibition zone around each disc was measured after 24 h for antibacterial activity and after 74 h for antifungal activity.

### 2.6. DNA cleavage studies

The DNA cleavage experiment was conducted using CT DNA by gel electrophoresis method. Cleavage reactions were run between the metal complexes and the DNA, and the solutions were diluted with loading dye using 1% agarose gel. Buffer solutions of 50 mmol tris-HCl/18 mmol NaCl in water (pH 7.1) and tris-acetic acid-EDTA in water (pH 8.3) were used, followed by the addition of 0.5 g of powdered agarose and mixed well. The solution was heated to boiling to dissolve agarose completely. The completely dissolved agarose gel solution was kept in the water bath at 65 °C. Then 3 µl of ethidium bromide (0.5 µg/ml) was added to the above solution and mixed well. The warmed agarose was poured and clamped immediately with comb to form sample wells. After setting (30–45 min. at room temperature) comb was removed and taped. The gel was mounted into electrophoretic tank. Enough electrophoretic buffers were added to cover the gel to a depth of about 1 mmol. The DNA sample (30 µm), 50 µm metal complex and 500 µm H<sub>2</sub>O<sub>2</sub> in tris-HCl/50 mmol NaCl buffer (pH 7.1) were mixed with loading dye and loaded into the well of the submerged gel using a micropipette. The electric current was passed into running buffer. The sample was running from negative to positive pole (Pelczar et al., 1998). After 1–2 h the gel was taken out from the buffer. After electrophoresis, the gel was photographed under UV transilluminator.

## 3. Results and discussion

### 3.1. Synthesis and characterization of ligand

Schiff base ligand is light yellow in colour and it is soluble in common organic solvents. The Schiff base formed was characterized with respect to its composition by elemental and spectral analysis. The physical characterization and its analytical data are given in Table 1. Elemental analysis data of the ligand show good agreement with theoretical values.

In the IR spectrum of indal-glygly, the characteristic stretching frequency of the azomethine group, (C=N) has occurred at 1618 cm<sup>-1</sup> and the  $\nu_{\text{asym}}(\text{COO}^-)$  and  $\nu_{\text{sym}}(\text{COO}^-)$  have appeared, respectively at 1587 and 1384 cm<sup>-1</sup>. The amide band of the potassium salt of the Schiff base ligand was seen at 1532 cm<sup>-1</sup>. The imine (N-H) stretching frequency of glygly at 3100 cm<sup>-1</sup> and carbonyl oxygen (C=O) stretching frequency of indal at 1700 cm<sup>-1</sup> have disappeared in the Schiff base ligand. This confirms the formation of indal-glygly from indal and glygly. The electronic spectrum of indal-glygly ligand exhibits an absorption band at 307 nm, which can be attributed to the  $\pi$ - $\pi^*$  transition of the azomethine chromophore.

<sup>1</sup>H NMR spectrum of indal-glygly shows the azomethine proton (-HC=N-) signal at 8.2 ppm and amide proton (-CONH-) signal at 7.6 ppm. The (-NH-) proton of indole ring shows the signal at 10.3 ppm and aromatic protons show the multiplet (aromatic-CH=CH-) at ~7.4–8.0 ppm. The two aliphatic protons (aliphatic-CH<sub>2</sub>-) in the chain show the multiplet signal at ~3.8–4.2 ppm.

The fast atom bombardment mass spectrum of indal-glygly recorded at room temperature shows the fragmentation pattern with the base peak (M<sup>+</sup>) at  $m/z = 259$  (C<sub>13</sub>H<sub>12</sub>N<sub>3</sub>O<sub>3</sub><sup>+</sup>). The fragments at  $m/z = 143$  and 116 corresponds, respectively to C<sub>11</sub>H<sub>9</sub>N<sub>2</sub>O<sup>+</sup> and C<sub>9</sub>H<sub>7</sub>N<sub>2</sub><sup>+</sup>. Based on the above studies, the proposed structure of indal-glygly is given in Fig. 1. The Schiff base ligand can bind the metal ion through azomethine, peptide and carboxylato groups.

### 3.2. Synthesis and characterization of metal complexes

The complexes are stable in air and atmosphere. All the complexes are soluble in DMSO, but they are insoluble in some common organic solvents. The analytical data (Table 1) indicate that the metal to ligand ratio is 1:1 in all the complex systems and it can be represented as [ML(H<sub>2</sub>O)]NO<sub>3</sub>, where L = indole-3-carboxaldehyde-glycylglycine(indal-glygly); M = Co(II), Ni(II) and Cu(II). The molar conductivity of metal complexes in DMSO solution (10<sup>-3</sup> M) at room temperature was measured to establish the charge of the metal complexes. The high molar conductance values (Table 1) indicate that

**Table 1** Analytical and physical data of Schiff base ligand and its complexes.

Compounds	Formula	Colour	Analytical (%) calculated (found)				Molar conductance (Ω <sup>-1</sup> cm <sup>2</sup> mol <sup>-1</sup> )
			C	H	N	M	
K[L]	KC <sub>13</sub> H <sub>12</sub> N <sub>3</sub> O <sub>3</sub>	Yellow	52.51 (52.35)	4.07 (4.05)	14.13 (14.08)	–	–
[CoL(H <sub>2</sub> O)]NO <sub>3</sub>	CoC <sub>13</sub> H <sub>14</sub> N <sub>4</sub> O <sub>7</sub>	Pink	39.31 (39.71)	3.55 (3.20)	14.11 (14.55)	14.84 (14.54)	69.81
[NiL(H <sub>2</sub> O)]NO <sub>3</sub>	NiC <sub>13</sub> H <sub>14</sub> N <sub>4</sub> O <sub>7</sub>	Pale green	39.33 (39.69)	3.55 (3.18)	14.11 (14.76)	14.78 (14.48)	70.72
[CuL(H <sub>2</sub> O)]NO <sub>3</sub>	CuC <sub>13</sub> H <sub>14</sub> N <sub>4</sub> O <sub>7</sub>	Blue	38.86 (38.64)	3.51 (3.16)	13.94 (13.67)	15.81 (15.91)	73.32

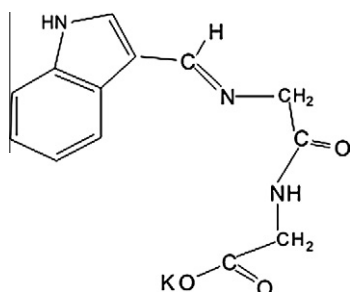


**Figure 1** Proposed structure of Schiff base ligand.

all the metal complexes behave as 1:1 electrolytes (Geary, 1971) as evidenced by the non-involvement of the nitrate group in coordination.

### 3.2.1. Infrared spectral studies

The Schiff base ligand shows  $\nu(\text{C}=\text{N})$  azomethine band at  $1618\text{ cm}^{-1}$ . On complexation, this band was shifted to lower frequency values in all the complexes (Table 2). It indicates that the azomethine nitrogen is coordinated to the metal ions (Nakamoto, 1997). In the spectrum of Schiff base ligand, the peptide band appeared at  $1532\text{ cm}^{-1}$ . On complexation, this band was shifted to lower frequency values (Table 2) indicating the linkage between metal ion and the peptide nitrogen atom (Nakamoto, 1997). The asymmetric carboxyl  $\nu_{\text{asym}}(\text{COO}^-)$  was shifted to higher frequency region and the symmetric carboxyl  $\nu_{\text{sym}}(\text{COO}^-)$  was shifted to lower frequency region (Table 2), indicating the linkage between the metal ion and carboxylato oxygen atom (Deacon and Phillips, 1980; Szorcisk et al., 2004). The  $\nu_{\text{asym}}(\text{COO}^-)$  and  $\nu_{\text{sym}}(\text{COO}^-)$  of the carboxylato group in the complexes show the separation value ( $\Delta\nu$ ) greater than  $200\text{ cm}^{-1}$ . This indicates monodentate binding of the carboxylato group in Co(II), Ni(II) and Cu(II) complexes (Grag et al., 2005). Furthermore, the presence of coordinated water molecules as evidenced by broad bands appeared at  $3389\text{--}3415\text{ cm}^{-1}$  in complexes may be attributed to O–H stretching vibration as supported from the thermal analysis (Mohamed et al., 2005). The IR spectra of the complexes show the bands appeared at  $1361\text{--}1371\text{ cm}^{-1}$ , which can be ascribed to the presence of free  $\text{NO}_3$  group (Khalil, 2000). The appearance of two bands at  $519\text{--}534$  and  $417\text{--}449\text{ cm}^{-1}$  correspond to  $\nu(\text{M}\text{--}\text{O})$  and  $\nu(\text{M}\text{--}\text{N})$  vibrations, (El-Jouad et al., 2001), respectively.

Thus the IR spectrum indicates that the Schiff base ligand (Fig. 1) in all the complexes under investigation is tridentate and the binding sites are azomethine nitrogen, peptide nitrogen and carboxylato oxygen atoms in all the three M(II)–indal-glygly complexes. The fourth position in the coordination sphere would be completed by water molecule.

### 3.2.2. Electronic spectral measurements

The UV–Visible spectrum of the Schiff base ligand exhibits an absorption band at  $307\text{ nm}$  in DMSO solution, which can be attributed to  $\pi\text{--}\pi^*$  transition of the azomethine chromophore. On complexation, this band was shifted to lower wavelength region, suggesting the coordination of azomethine nitrogen with the metal ions (Lever, 1968).

The spectrum of Co(II) complex of indal-glygly shows a peak with  $\lambda_{\text{max}}$  value of  $625\text{ nm}$ . This is due to the tetrahedral environment of the ligand around the metal ion due to  $^4\text{A}_2(\text{F}) \rightarrow ^4\text{T}_1(\text{P})$  transition. Hence, Co(II) complex can be assigned tetrahedral geometry. The spectrum of Ni(II) complex of indal-glygly shows an absorption band at  $582\text{ nm}$ . This peak corresponds to the transition  $^3\text{T}_1(\text{F}) \rightarrow ^3\text{T}_1(\text{P})$  which indicates the tetrahedral environment of the ligand surrounding Ni(II) in the complex (Lever, 1968). In general, due to Jahn–Teller distortion, square planar Cu(II) complexes give a broad absorption band between  $600$  and  $700\text{ nm}$ . The present Cu(II) complex shows the band at  $681\text{ nm}$  suggesting the complex to have square planar geometry.

### 3.2.3. Magnetic susceptibility measurements

The observed magnetic moment value of the Co(II)–indal-glygly complex is  $4.66\text{ BM}$ . This is the expected value of  $4.2\text{--}4.88\text{ BM}$  for the tetrahedral Co(II) complexes, which is the sum of contributions due to spin only moments and spin–orbit coupling. Thus, the Co(II)–indal-glygly complex shows the tetrahedral geometry. The magnetic moment value of  $3.57\text{ BM}$  for the Ni(II)–indal-glygly complex is in the range of  $3.2\text{--}4.0\text{ BM}$  expected for the tetrahedral Ni(II) complexes. Cu(II) square planar complexes exhibit magnetic moments in the range  $1.8\text{--}2.1\text{ BM}$ . These values are slightly higher than the spin only value of  $1.73\text{ BM}$  and this is due to the spin–orbit coupling followed by lowering of symmetry (Banerjee, 1993). The magnetic moment obtained for Cu(II)–indal-glygly complex is  $1.81\text{ BM}$ , which is characteristic for the square planar geometry of the Cu(II) complexes.

The vibrating sample magnetometer measurements (Fig. 2a and b) shows the plot of magnetization (M) as a function of applied field (H) for the Co(II) and Ni(II) complexes. The plots show the hysteresis loop for complexes at room temperature and give a saturation magnetization of  $0.25\text{ emu/g}$ . The coercivities of the Co(II) and Ni(II) complexes were  $340$  and  $706\text{ Oe}$ , respectively. The low saturation magnetization and the presence of coercivities for the samples indicate that these complexes are weakly ferromagnetic (Cullity, 1972). But Cu(II) complex did not show any hysteresis loop at room temperature indicating that the Cu(II) complex is paramagnetic (Cullity, 1972; Joseph et al., 2005) in nature.

### 3.2.4. Electron spin resonance spectra

The ESR spectra of the Cu(II) complex recorded in DMSO at  $300$  and  $77\text{ K}$  are shown in Fig. 3a and b. The spectrum re-

**Table 2** IR spectral data ( $\text{cm}^{-1}$ ) of Schiff base ligand and its complexes.

Compound	$\nu(\text{C}=\text{N})$	$\nu(\text{O}\text{--}\text{H})$	$\nu(\text{peptide})$	$\nu_{\text{asym}}(\text{COO}^-)$	$\nu_{\text{sym}}(\text{COO}^-)$	$\nu(\text{M}\text{--}\text{N})$	$\nu(\text{M}\text{--}\text{O})$
K[L]	1618	3364	1532	1591	1386	–	–
[CoL(H <sub>2</sub> O)]NO <sub>3</sub>	1607	3415	1527	1593	1385	522	443
[NiL(H <sub>2</sub> O)]NO <sub>3</sub>	1612	3393	1526	1596	1381	519	417
[CuL(H <sub>2</sub> O)]NO <sub>3</sub>	1608	3389	1523	1590	1382	524	435

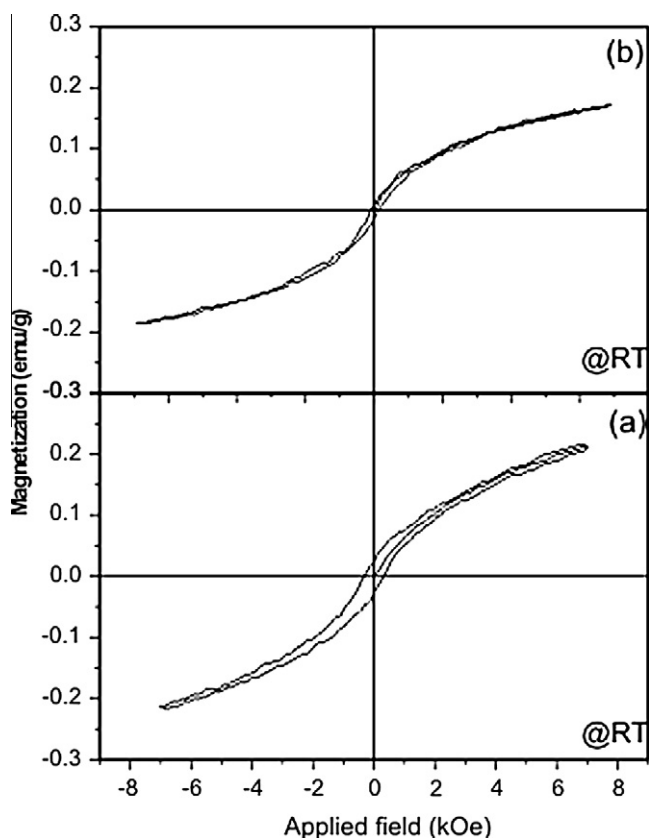


**Figure 2** Magnetization versus applied field plots for (a) Co(II) and (b) Ni(II) Schiff base complexes.

corded at 300 K shows one intense absorption band at high field, which is isotropic due to the tumbling motion of the molecules. However, this complex in the frozen state shows four well resolved peaks with low intensities in the low field region and one intense peak in the high field region. The magnetic susceptibility of 1.81 BM for the Cu(II)-indal-glygly complex indicates the presence of one unpaired electron, showing the complex to be mononuclear in nature. This fact is also evident from the absence of a half field signal, observed in the ESR spectrum at 1600 G due to the  $m_s = \pm 2$  transitions, ruling out any Cu-Cu interaction (Farmer and Urbach, 1974; Ray and Kantiman, 1990; Antosik et al., 1969; Ismail, 2005). For the present Cu(II) complex, the observed  $g$  values are  $g_{\parallel}$  (2.45) >  $g_{\perp}$  (2.13) >  $g_e$  (2.0023), suggesting the unpaired electron to be in the  $d_{x^2-y^2}$  orbital and the complex is square planar.

In the axial spectra, the  $g$ -values are related with exchange interaction coupling constant ( $G$ ). The observed value of 3.5 for  $G$  in the present copper complex suggests that significant exchange coupling is present and the misalignment is appreciable, and the unpaired electron is present in the  $d_{x^2-y^2}$  orbital. This result also indicates that the exchange coupling effects are not operative in the present complex. It is usual to determine the covalent bonding parameters for Cu(II) in various ligand field environments. In a square planar Cu(II) complex, the unpaired electron resides in the  $d_{x^2-y^2}$  orbital and  $g_{\parallel}$  and  $g_{\perp}$  are given in the order  $g_{\parallel} > g_{\perp} > 2$ . When the unpaired electron is in the  $d_z^2$  orbital  $g_{\parallel}$  and  $g_{\perp}$  are given in the order

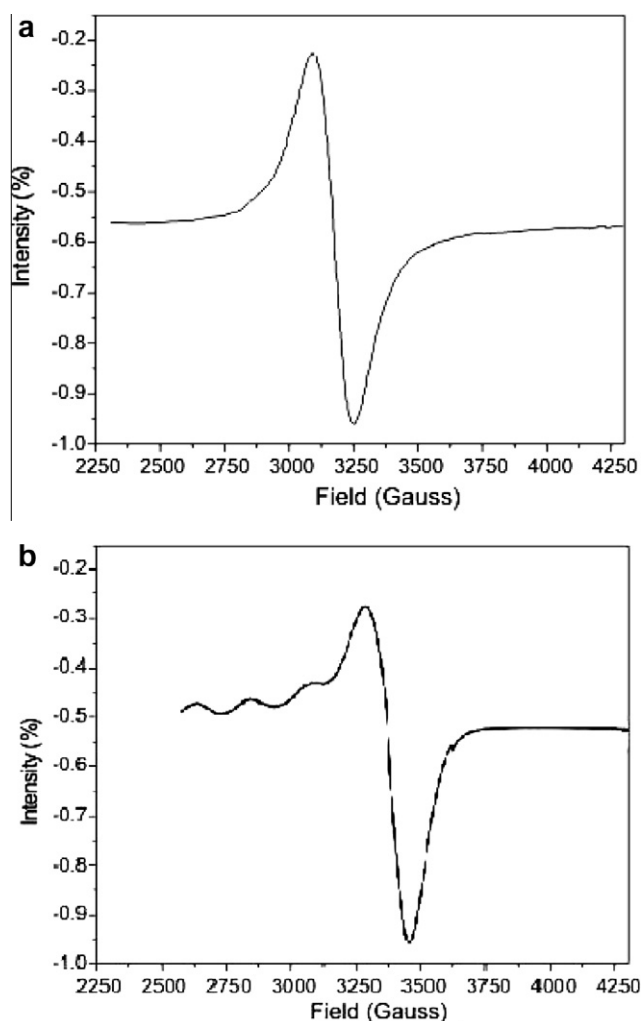


**Figure 3** ESR spectra of Cu(II) Schiff base complexes at (a) 300 K and (b) 77 K.

$g_{\perp} > g_{\parallel} > 2$ . The exchange interaction coupling constant  $G$  is calculated from Eq. (1).

$$G = (g_{\parallel} - 2)/(g_{\perp} - 2). \quad (1)$$

According to Hathaway (Hathaway and Tomlinson, 1970), if  $G > 4.0$ , the local tetragonal axes are aligned parallel or only slightly misaligned. If  $G < 4.0$ , significant exchange coupling is present and the misalignment is appreciable. The in-plane  $\sigma$ -bonding covalency parameters (Fidone and Stevens, 1959),  $\alpha^2$  are related to  $g_{\parallel}$  and  $g_{\perp}$  according to Eq. (2).

$$\alpha^2 = -(A_{\parallel}/0.036) + (g_{\parallel} - 2.0036) + 3/7(g_{\perp} - 2.0036) + 0.04 \quad (2)$$

The  $\alpha^2$  value of 0.5 indicates complete covalent bonding, while that of 1.0 suggests complete ionic bonding. The out-of-plane  $\pi$ -bonding ( $\gamma^2$ ) and in-plane  $\pi$ -bonding ( $\beta^2$ ) parameters are calculated using Eqs. (3) and (4).

$$\beta^2 = (g_{\parallel} - 2.0036)E / -8\lambda\alpha^2 \quad (3)$$

$$\gamma^2 = (g_{\perp} - 2.0036)E / -2\lambda\alpha^2, \quad (4)$$

**Table 3** Electrochemical data of the Schiff base metal complexes.

Compound	Couple	$E_{pc}$ (V)	$E_{pa}$ (V)	$i_{pc}$ ( $\mu$ A)	$i_{pa}$ ( $\mu$ A)
[CoL(H <sub>2</sub> O)]NO <sub>3</sub>	Co(II)/Co(I)	-0.720	–	15.0	–
[NiL(H <sub>2</sub> O)]NO <sub>3</sub>	Ni(II)/Ni(I)	–	0.740	–	3.0
[CuL(H <sub>2</sub> O)]NO <sub>3</sub>	Cu(II)/Cu(I)	-0.730	-0.620	12.5	9.2

Here,  $\lambda = -828 \text{ cm}^{-1}$  for free Cu(II) ion and  $E$  is the electronic energy for  ${}^2B_{1g} \rightarrow {}^2A_{1g}$  transition. This is also confirmed by orbital reduction factors  $K$ , which can be estimated using Eqs. (5) and (6).

$$K_{\parallel} = \alpha^2 \beta^2 \quad (5)$$

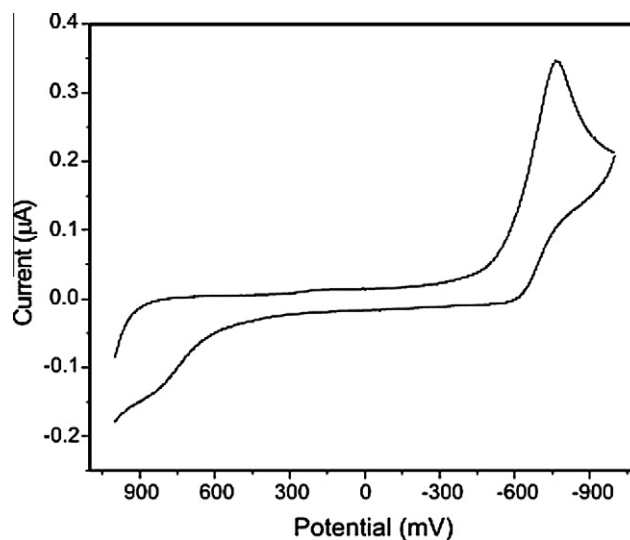
$$K_{\perp} = \alpha^2 \gamma^2 \quad (6)$$

Significant information about the nature of bonding in the Cu(II) complex can be derived from the relative magnitudes of  $K_{\parallel}$  and  $K_{\perp}$ . In the case of pure  $\sigma$ -bonding,  $K_{\parallel} \approx K_{\perp} = 0.77$ , whereas  $K_{\parallel} < K_{\perp}$  implies considerable in-plane  $\pi$ -bonding, while for out-of-plane  $\pi$ -bonding  $K_{\parallel} > K_{\perp}$ . Molecular orbital coefficients  $\alpha^2$  (in-plane  $\sigma$ -bonding),  $\beta^2$  (in-plane  $\pi$ -bonding) and  $\gamma^2$  (out-of-plane  $\pi$ -bonding) were calculated using the Eqs. (2)–(4). The observed  $\alpha^2$  value (0.916) indicates that Cu(II) complex is predominantly ionic in character. The observed  $\beta^2$  value (1.17) and  $\gamma^2$  value (1.32) shows that there is interaction in the out-of-plane  $\pi$ -bonding, whereas the in-plane  $\pi$ -bonding is predominantly ionic. This is also confirmed by orbital reduction factors (West, 1984) which were estimated from the simple relations. For the present complex, the observed order  $K_{\perp}(1.21) > K_{\parallel}(1.07)$  implies a greater contribution from in-plane  $\pi$ -bonding than for out-of-plane  $\pi$ -bonding in metal–ligand  $\pi$ -bonding. Thus, the ESR study of the copper complex has provided supporting evidence for the optical results.

### 3.2.5. Electrochemical studies

The electrochemical behaviour of the Co(II), Ni(II) and Cu(II) complexes were examined in DMSO solution at 0.1 V s<sup>-1</sup> scan rate and the results are summarized in Table 3. The cobalt complex shows (Table 3) an irreversible peak at -0.720 V which is attributed to Co(II)/Co(I) couple. The nickel complex also shows (Table 3) an irreversible peak at 0.740 V. This is due to Ni(II)/Ni(I) couple.

The cyclic voltammogram of Cu(II) complex (Fig. 4) in DMSO solution at 300 K in the potential range +0.2 to -1.2 V and at scan rate 0.1 V s<sup>-1</sup> was recorded. It shows a well defined redox process corresponding to the quasi-reversible Cu(II)/Cu(I) couple. The anodic peak at  $E_{pa} = -0.730$  V versus Ag/AgCl and the associated cathodic peak at  $E_{pc} = -0.620$  V correspond to the Cu(II)/Cu(I) couple. The Cu(II) complex exhibits a quasi-reversible behaviour as indicated by the non-equivalent current intensity of cathodic and anodic peaks and a peak separation,  $\Delta E_p$  value of 110 mV. The quasi-reversibility of the Cu(II)/Cu(I) couple was checked by varying the scan rates with peak potentials (Long et al., 1999; Arslan et al., 2002). The complex is found to be stabilized in the unusual oxidation state of copper in its +1 oxidation state during electrolysis. These observations suggest that indolglygly can stabilize Cu(I) ion probably because of its indole group having  $\pi$  back bonding effect (Bottcher et al.,

**Figure 4** Cyclic voltammogram of Cu(II) Schiff base complex.

1997). These observations suggested that the ligand can stabilize the unusual oxidation states of Co(I) and Ni(I) for cobalt and nickel complexes during electrolysis whereas Cu(III) for copper complex.

### 3.2.6. Thermal studies

The thermal behaviour of the complexes has been studied using TGA and DSC analysis.

**3.2.6.1. TGA analysis.** The thermal decomposition results of Cu(II) complex takes place in three stages. The first stage of decomposition is noticed in the temperature range 120–135 °C. It is due to the elimination of coordinated water molecule (Vargova et al., 2004). The mass loss observed in this step is 4.45% against the calculated loss of 4.37%. The second stage of decomposition occurs in the temperature range of 210–235 °C, due to melting and partial decomposition of the ligand, this step bringing the weight loss of 17% (calc. 17.76%). The decomposition range (310–335 °C) of weight loss in third stage gives 70% (calc. 70.21%). This is due to the decomposition of the ligand molecule. The complex is present in the form of its metal oxide above 400 °C.

**3.2.6.2. DSC analysis.** The DSC curve of the Cu(II) complex (Fig. 5b) shows an exothermic peak at ~125 °C due to the evaporation of the coordinated water molecule. Another sharp endothermic peak at 215 °C is noticed probably due to the melting and partial decomposition of the complex. The broad exothermic peak in the temperature region 320–330 °C is due to the final decomposition of the complex. The final residue

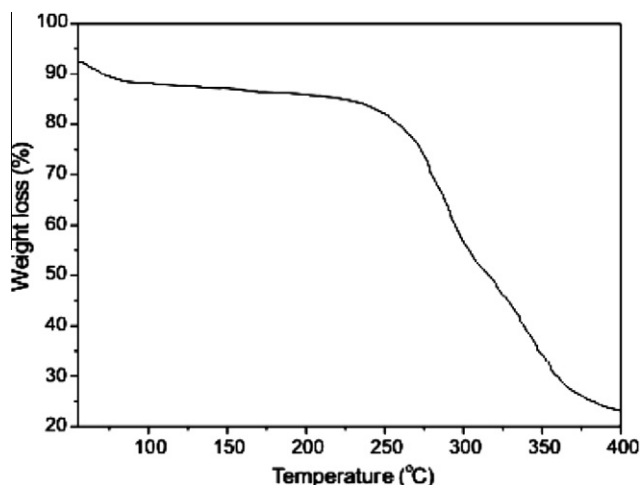


Figure 5a TGA curve of Cu(II) Schiff base complex.

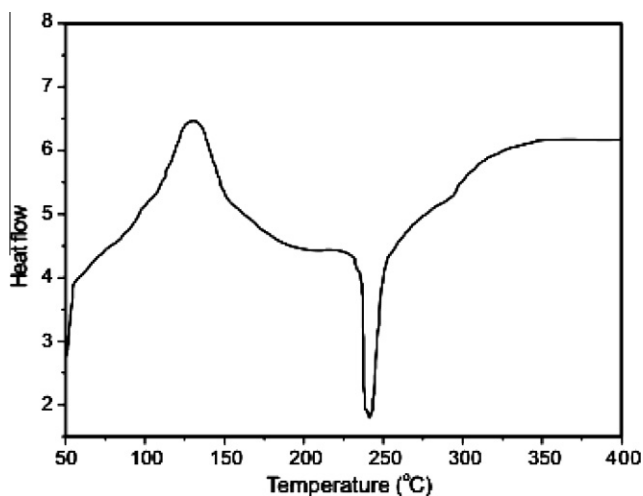


Figure 5b DSC curve of Cu(II) Schiff base complex.

in the complex above 400 °C is the metal oxide in keeping with the observation made in the case of monomeric systems. Similar type of TGA and DSC results (Table 4) were obtained for Co(II) and Ni(II) complexes.

### 3.2.7. X-ray diffraction studies

XRD pattern of the Co(II), Ni(II) and Cu(II) complexes are shown in Figs. 6(a–c). The XRD pattern of the metal com-

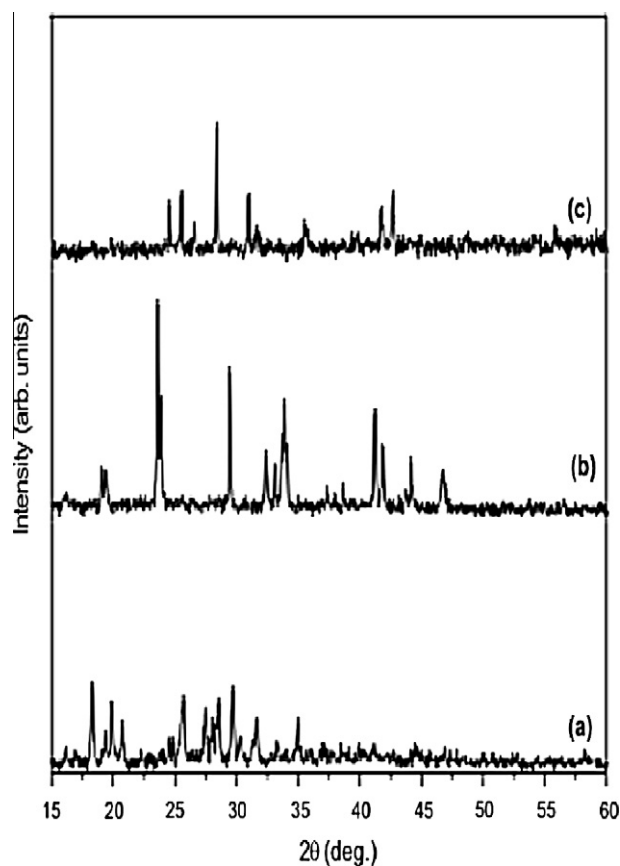


Figure 6 XRD pattern of (a) Co(II), (b) Ni(II) and (c) Cu(II) Schiff base complexes.

plexes shows well defined crystalline peaks indicating that the samples were crystalline in phase (Souaya et al., 2000; Yacob, 2005). The metal complexes show sharp crystalline XRD patterns, which differ considerably from that of the ligand. The appearance of crystallinity in the metal–Schiff base complexes is due to the inherent crystalline nature of the metallic compounds. The grain size of the metal Schiff base complexes,  $d_{\text{XRD}}$  was calculated using Scherrer's formula (Cullity, 1978) by measuring the full width at half maximum of the XRD peaks.

$$d_{\text{XRD}} = 0.9\lambda/\beta(\text{Cos}\theta),$$

where ' $\lambda$ ' is the wavelength, ' $\beta$ ' is the full width at half maximum and ' $\theta$ ' is the peak angle. The complexes have the average

Table 4 Thermoanalytical results of Schiff base metal complexes.

Compound	Temperature range (°C)	Loss in weight found (calc.) (%)	DSC peak (°C)	$\Delta H$ (J g <sup>-1</sup> )	Assignments
[CoL(H <sub>2</sub> O)]NO <sub>3</sub>	50–136	9.2 (9.17)	149	87.79	H <sub>2</sub> O
	136–285	8.89 (8.86)	181	54.27	Ligand
	287–397	81.68 (81.43)	381	–79.85	CoO
[NiL(H <sub>2</sub> O)]NO <sub>3</sub>	50–141	6.6 (6.17)	117	67.92	H <sub>2</sub> O
	141–246	16.27 (16.76)	159	28.27	Ligand
	246–400	77.07 (77.21)	384	–92.52	NiO
[CuL(H <sub>2</sub> O)]NO <sub>3</sub>	50–164	5.5 (5.17)	134	94.01	H <sub>2</sub> O
	164–260	17 (17.76)	250	–42.70	Ligand
	260–400	77 (77.21)	391	73.79	CuO

crystallite size of 31, 40 and 67 nm, respectively suggesting that the complexes are nanocrystalline.

### 3.2.8. Scanning electron microscope

The SEM micrographs of the Co(II), Ni(II) and Cu(II) complexes are shown in Figs. 7a–c, respectively. It is seen from the figures that the Co(II) and Ni(II) complexes shows platelet-like structure, while Cu(II) complex exhibit the cauliflower-like structure. The particle sizes of the Co(II), Ni(II) and Cu(II)–indal-glygly complexes were in the diameter range of few microns. However, particles with size less than 100 nm were also observed which groups to form agglomerates of larger size. The average crystallite size obtained from XRD also shows that the particles were agglomerated that these complexes have polycrystalline with nanosized grains.

### 3.3. Antimicrobial studies

The antibacterial and antifungal activities of the Schiff base ligand and its Co(II), Ni(II) and Cu(II) complexes were compared with standard antibiotics like *Amikacin*, *Ofloxacin*, *Ciprofloxacin* and *Nystatin*. The antibacterial and antifungal results are summarized in the Table 5a and b. The antibacterial and antifungal activity of the ligand and its metal complexes indicate that the complexes possess higher growth inhibition potential compared to those of the ligand. The antimicrobial

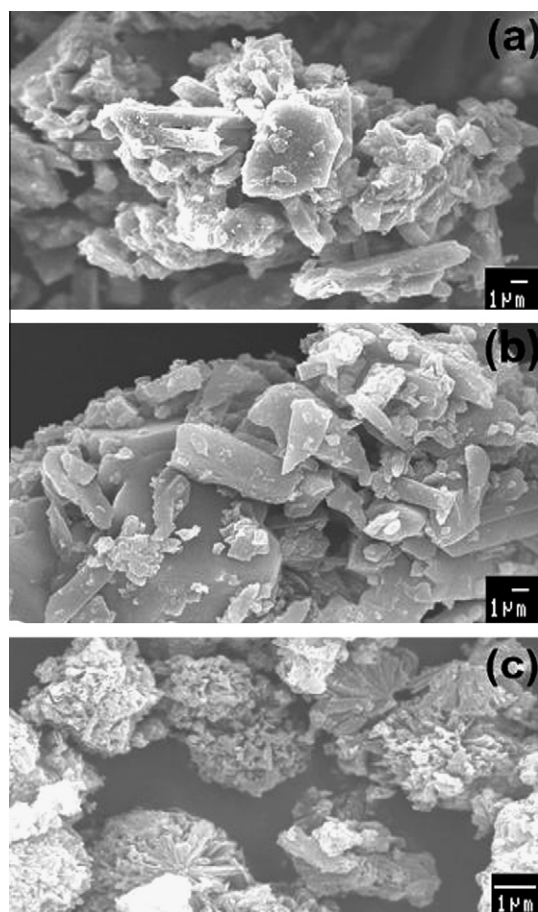


**Figure 7** SEM images of (a) Co(II), (b) Ni(II) and (c) Cu(II) Schiff base complexes.

activity of the metal complexes increases with increase in concentration of the complexes. It is suggested that the complexes having antibacterial and antifungal activities inhibit multiplication process of the microbes by blocking their active sites (Sari et al., 2003; Mohamed, 2006; Mishra and Singh, 1993).

The mechanism of toxic activity of the complexes with the ligands can be ascribed to the increase in the lipophilic nature of the complexes arising from chelation. Chelation reduces the polarity of the metal atom mainly because of partial sharing of its positive charge with the donor groups and possible  $\pi$  electron delocalization within the whole chelate ring. The chelation also increases the lipophilic nature of the central metal atom, which subsequently favours the permeation through the lipid layer of cell membrane. The mode of action of complexes involves the formation of hydrogen bonds with the imino group by the active sites leading to interference with the cell wall synthesis (Bayer et al., 1996). This hydrogen bond formation damages the cytoplasmic membrane and the cell permeability may also be altered leading to cell death.

The bioactivity of the ligand and its complexes is found to be in the order: Cu(II) > Co(II) > Ni(II) > indal-glygly. The difference in antimicrobial activity is due to the nature of metal ions and also the cell membrane of the microorganisms. The higher bioactivity of the complexes compared to that of the ligand is due to the decrease in the charge localization of the metal ion that leads to more lipid solubility. The higher activity of Cu(II) complexes can be explained as, on chelation the polarity of Cu(II) ion is found to be reduced to a greater extent due to the overlap of the ligand orbital and partial sharing of the positive charge of the copper ion with donor groups. Therefore, Cu(II) ions are adsorbed on the surface of the cell wall of microorganisms (Ferrari et al., 1999; Wahab et al., 2004). The adsorbed Cu(II) ions disturb the respiratory process of the cells, thus blocking the synthesis of proteins. This, in turn, restricts further growth of the organisms.

### 3.4. DNA cleavage studies

There are a number of agents, which exert their effect by inhibiting enzymes that act upon DNA. These inhibitions result from the binding of agents to the enzyme's site of interaction on DNA. Transition metals have been seen to inhibit DNA repair enzymes. When DNA is run on horizontal gel using electrophoresis, the fastest migration will be observed for the open circular form (Form I). If one strand is cleaved a slower-moving linear form (Form II) is observed. Gel electrophoretic experiment using CT DNA was performed with metal complexes at 35 °C in the presence of H<sub>2</sub>O<sub>2</sub> as oxidant. The DNA cleavage efficiency of the complex was due to the different binding affinity of the complex to DNA. Control experiment using DNA alone (Lane 1) does not show any significant cleavage even on longer exposure time (Pelczar et al., 1998).

The results (Fig. 8a) indicate that the present copper complex (Lane 4) can cleave DNA effectively compared to other complexes. The other complexes do not cleave DNA in the presence of H<sub>2</sub>O<sub>2</sub>. Probably this is due to the formation of redox couple of the metal ions and its behaviour. The redox cycling between Cu(II) and Cu(I) can catalyze the production of highly reactive hydroxyl radicals. These hydroxyl radicals (Pelczar et al., 1998) participate in the oxidation of the deoxyribose moiety, followed by hydrolytic cleavage of the sugar-phos-

phate backbone. It is observed that most cleavage cases are caused by copper ions reacting with  $H_2O_2$  to produce the diffusible hydroxyl radical or molecular oxygen, which may dam-

age DNA through Fenton type chemistry. Further, the presence of a smear in the gel diagram indicates the presence of radical cleavage.

**Table 5a** Antibacterial activity of Schiff base ligand and its complexes.

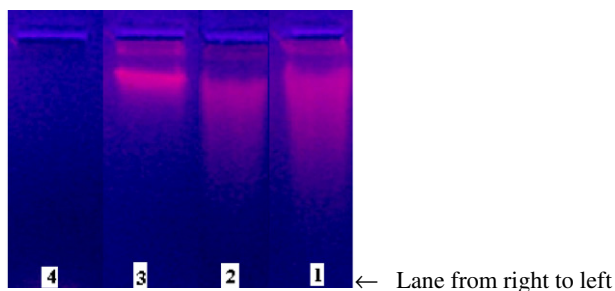
Compounds	Gram positive bacteria		Gram negative bacteria		
	<i>S. aureus</i>	<i>K. pneumoniae</i>	<i>P. vulgaris</i>	<i>E. coli</i>	<i>P. aeruginosa</i>
K[L]	5	3	6	4	10
[CoL(H <sub>2</sub> O)]NO <sub>3</sub>	27	24	18	14	20
[NiL(H <sub>2</sub> O)]NO <sub>3</sub>	18	22	15	10	14
[CuL(H <sub>2</sub> O)]NO <sub>3</sub>	34	28	22	24	28
Amikacin <sup>a</sup>	36	38	40	44	48
Ofloxacin <sup>a</sup>	42	40	38	32	36
Ciprofloxacin <sup>a</sup>	38	30	28	24	34

<sup>a</sup> Standards (the tested compounds were prepared in DMSO and the concentration used in this study was 0.01  $\mu$ g/ml. Bacterial activity was measured in mm diameter in agar plates).

**Table 5b** Antifungal activity of Schiff base ligand and its complexes.

Compounds	<i>C. albicans</i>	<i>R. stolonifer</i>	<i>A. niger</i>	<i>A. flavus</i>	<i>R. bataicola</i>
K[L]	6	12	10	8	4
[CoL(H <sub>2</sub> O)]NO <sub>3</sub>	18	22	20	22	16
[NiL(H <sub>2</sub> O)]NO <sub>3</sub>	12	18	16	20	10
[CuL(H <sub>2</sub> O)]NO <sub>3</sub>	26	32	28	30	20
Nystatin <sup>a</sup>	30	38	42	36	28

<sup>a</sup> Standard (the tested compounds were prepared in DMSO and the concentration used in this study was 0.01  $\mu$ g/ml. Fungal activity was measured in mm diameter in agar plates).



Lane 1: Control DNA; Lane 2: DNA + Co(II) complex +  $H_2O_2$ ;  
Lane 3: DNA + Ni(II) complex +  $H_2O_2$  and Lane 4: DNA + Cu(II) complex +  $H_2O_2$

**Figure 8a** Agarose gel (1%) showing the results of electrophoresis of CT DNA with Schiff base metal complexes.

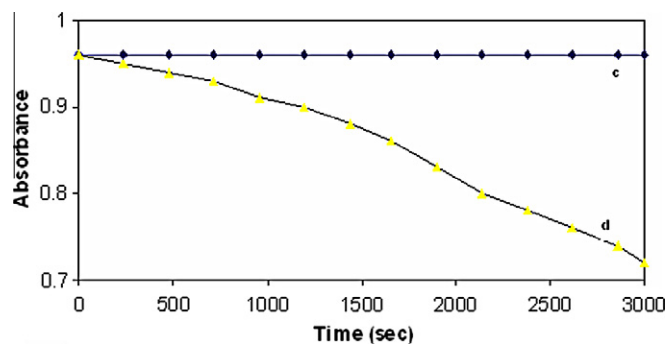


**Figure 8b** Rhodamine B degradation followed by decrease of absorbance at 552 nm, pH 8.1 in 10 mmol phosphate buffer: (c) in presence of 0.1 mmol Cu(II) complex and (d) in presence of 0.1 mmol Cu(II) complex, 1 mmol  $H_2O_2$  and 10 mmol ascorbic acid.

### 3.5. Investigation of the active oxygen species

In the presence of reactive oxygen donor species, copper is thought to be able to form different intermediates, depending on the specific complex and conditions. A non-diffusible copper–oxene intermediate has been invoked in some cleavage reactions, while in others Fenton-type chemistry which involves release of diffusible hydroxyl radicals has been suggested. In order to study the active species, standard scavengers of reactive oxygen intermediates were included in the electrophoretic studies. To understand the active oxygen species in the reactions, inhibition experiments were carried out with standard scavengers for reactive oxygen intermediates and degradation experiments with Rhodamine B dye (552 nm). The degradation of the dye provides a direct measure of the concentrations of hydroxyl radicals (Fig. 8b) in the reaction mixture. From the observation, it is suggested that reactive oxygen species can be produced by the copper complex in the presence of oxidant.

### 4. Conclusion

Co(II), Ni(II) and Cu(II) complexes of the Schiff base ligand derived from glycylglycine and indole-3-carboxaldehyde were synthesized and characterized. Conductance measurements indicated that the complexes are 1:1 electrolytes. The results clearly demonstrate that the Schiff base ligand is tridentate, Co(II) and Ni(II) complexes have tetrahedral geometry, while the Cu(II) complex has square planar geometry. IR and thermal studies indicated that the fourth position would be occupied by a water molecule in complexes. XRD pattern of the complexes showed the crystallite size of 31, 40 and 67 nm, respectively. The surface morphology using SEM showed that the particles were agglomerated in all the complexes. The antimicrobial activity of the ligand and its complexes indicate that the Cu(II) complexes possess high bacterial and fungal activities than the other complexes and ligand. Such activity is explained on the basis of chelation theory and overtones concept. Copper ions are proved to be essential for the growth-inhibitor effect. The extent of inhibition appeared to be strongly dependent on the initial cell density and on the growth medium. Gel electrophoretic experiment using CT DNA were performed with metal complexes in the presence of H<sub>2</sub>O<sub>2</sub> as an oxidant. In order to study the active species, standard scavengers of reactive oxygen intermediates were included in the electrophoretic studies.

### Acknowledgement

We thank the Department of Nuclear Physics, University of Madras, Guindy Campus, Chennai, India for extending their research facilities to carry part of this study.

### References

- Antosik, S., Brown, N.M.D., Meconnel, A.A., Potte, A.L., 1969. *J. Chem. Soc. A*, 545.
- Arslan, H., Pozan, N.O., Tarkan, N., 2002. *Thermochim. Acta* 383, 69.
- Banerjea, D., 1993. *Coordination Chemistry*. Tata McGraw-Hill Publisher.
- Bayer, A.W., Kirby, M.M.W., Sherries, J.C., Truck, M., 1996. *Am. J. Clin. Pathol.* 45, 493.
- Bottcher, A., Takeuchi, T., Hardcastle, K.I., Meade, T.J., Gray, H.B., 1997. *Inorg. Chem.* 36, 2498.
- Colacio, E., Ghazi, M., Kivekas, M., Moreno, J.M., 2000a. *Inorg. Chem.* 39, 2882.
- Cullity, B.D., 1972. *Introduction to Magnetic Materials*. Addison-Wesley Publisher, London.
- Cullity, B.D., 1978. *Elements of X-ray Diffraction*, second ed. Addison-Wesley, Publisher, Philippines.
- De Souza, V.R., Numes, G.S., Rocha, R.C., Toma, H.F., 2003. *Inorg. Chim. Acta* 50, 348.
- Deacon, G.B., Phillips, R.J., 1980. *Coord. Chem. Rev.* 33, 227.
- El-Jouad, Riou, A., Allian, M., Khan, M.A., Bouet, G.M., 2001. *Polyhedron* 20, 67.
- Farmer, R.L., Urbach, F.L., 1974. *Inorg. Chem.* 13, 587.
- Ferrari, M.B., Capacchi, S., Reffo, G., Tarasconi, P., Albertini, R., Pinelli, S., Lunghi, P., 1999. *Inorg. Chim. Acta* 286, 134.
- Fidone, I., Stevens, K.W.H., 1959. *Proc. Phys. Soc. Lond.* 73, 116.
- Geary, W.J., 1971. *Coord. Chem. Rev.* 7, 81.
- Grag, B.S., Kumar, D.N., Sarbhai, M., 2005. *Spectrochim. Acta A* 61, 141.
- Hathaway, B.J., Tomlinson, A.A.G., 1970. *Coord. Chem. Rev.* 5, 1.
- Ismail, T.M.A., 2005. *J. Coord. Chem.* 58, 141.
- Joseph, D.P., Kumar, G.S., Venkateswaran, C., 2005. *Mater. Lett.* 59, 2720.
- Joseyphus, R.S., Dhanaraj, C.J., Nair, M.S., 2006. *Transition Met. Chem.* 31, 699.
- Joseyphus, R.S., Nair, M.S., 2008. *Mycobiology* 36 (2), 93.
- Kannan, S., Ramesh, R., 2005. *J. Coord. Chem.* 58 (7), 567.
- Karaliota, A., Kresti, O., Tzougraki, C., 2001. *J. Inorg. Biochem.* 84, 33.
- Khalil, S.M.E., 2000. *J. Coord. Chem.* 52, 73.
- Lever, A.B.P., 1968. *Inorganic Electronic Spectroscopy*, second ed. Elsevier, New York.
- Long, L.S., Yang, S.P., Chen, X.M., Tong, Y.X., Ln, J., 1999. *J. Chem. Soc., Dalton Trans.* 12, 1999.
- Mascharak, P.K., 2002. *Coord. Chem. Rev.* 225, 201.
- Mishra, L., Singh, V.K., 1993. *Indian J. Chem. A* 32, 446.
- Mohamed, G.G., 2006. *Spectrochim. Acta A* 64, 188.
- Mohamed, G.G., Omar, M.M., Hindy, A.M.M., 2005. *Spectrochim. Acta A* 62, 1140.
- Nair, M.S., Joseyphus, R.S., 2008. *Spectrochim. Acta A* 70, 749.
- Nair, M.S., Sudhakumari, S., Neelakantan, M.A., 2007. *J. Coord. Chem.* 60, 1291.
- Nakamoto, K., 1997. *Infrared and Raman Spectra of Inorganic and Coordination Compounds*, fifth ed. Wiley, New York.
- Pelczar, M.J., Chan, E.C.S., Krieg, N.R., 1998. *Microbiology*, fifth ed. New York.
- Przybylski, P., Jasinski, K., Brzezinski, B., Bartl, F., 2002. *J. Mol. Struct.* 611, 193.
- Ray, R.K., Kantiman, G.B., 1990. *Inorg. Chim. Acta* 173, 207.
- Sari, N., Arslan, S., Logolu, E., Sakiyan, I., 2003. *J. Sci.* 16, 283.
- Souaya, E.R., Hanna, W.G., Isamil, E., Milad, N., 2000. *Molecules* 5, 1121.
- Szorcisk, A., Nagy, L., Sletten, J., Szalontai, G., Kamu, E., Fiore, T., Pellerito, L., Vargova, Z., Zeleoak, V., Cisaoova, I., Gyoryova, K., 2004. *Thermochim. Acta* 423, 149.
- Vargova, Z., Zeleoak, V., Cisaoova, I., Gyoryova, K., 2004. *Thermochim. Acta* 423, 149.
- Vogel, A.I., 1978. *A Textbook of Quantitative Inorganic Analysis Including Elementary Instrumental Analysis*, fourth ed. Longman, London.
- Wahab, Z.H.A., Mashaly, M.M., Salman, A.A., El-Shetary, B.A., Faheim, A.A., 2004. *Spectrochim. Acta A* 60, 2861.
- West, D.S., 1984. *J. Inorg. Nucl. Chem.* 43, 3161.
- Yaacob, A.H.I., 2005. *Mater. Forum.* 29, 199.